Available online at www.sciencedirect.com
SCIENCE DIRECT®

Journal of the European Ceramic Society 23 (2003) 1881–1891
www.elsevier.com/locate/jeurceramsoc

NO_2 sensitivity of a heterojunction sensor based on WO_3 and doped SnO_2

Z. Ling, C. Leach*, R. Freer

Manchester Materials Science Centre, University of Manchester and UMIST, Manchester M1 7HS, UK

Received 13 September 2002; accepted 11 November 2002

Abstract

The NO_2 sensing properties of a heterojunction gas sensor formed between WO_3 and 3 wt.% Nd_2O_3 doped SnO_2 were evaluated using DC and AC measurements at 300 °C and compared with the responses obtained from single component tungsten oxide and doped tin oxide sensors. The heterojunction sensor showed rectifying behaviour with a forward bias direction defined as SnO_2^-/WO_3^+. The heterojunction sensor and the component materials were all found to be sensitive to NO_2, showing almost linear resistance increases with concentration when exposed to 0–5 ppm NO_2. However, the sensitivity of the heterojunction sensor was almost an order of magnitude greater than either of the component sensors. Under reverse bias the effective sensor resistance did not change with NO_2 concentration. AC impedance spectroscopy demonstrated that the improved NO_2 response of the heterojunction sensor occurred primarily as a result of increases in the forward bias resistance of the heterojunction interface. The long-term stability of the heterojunction sensor was characterised over 53 days using continuous DC resistance measurements, under an applied forward bias voltage of 0.4 V. The sensor showed good stability, with low drift and a reproducible response to NO_2 in the concentration range 0–10 ppm throughout the test period.

Keywords: Electrical properties; Heterojunction; Interfaces; Sensors; SnO_2/WO_3; Surfaces

1. Introduction

Since the discovery nearly half a century ago that the charge-carrier concentration on the surface of a semiconductor is sensitive to the composition of the surrounding atmosphere,[1] considerable research has been carried out on the development of novel solid-state gas sensors based on semiconducting metal oxides. As a result many such commercial gas sensors have been developed and marketed[2–5] and, with currently acceptable levels of performance, are used increasingly to monitor gases in various fields such as industrial and environmental control.[5,6]

In general, semiconducting gas sensors are single-phase ceramics that detect surface adsorbed gases through changes in surface conductivity as a result of electron transfer between the gas molecules and the sensor surface.[7] However, such sensors generally have disadvantages of poor selectivity, insensitivity to the very low gas concentrations required for certain applications and require periodic conditioning cycles to ensure consistency of performance.[8,9] Several different approaches have been explored in attempts to overcome these and related issues, many of which have involved the use of secondary reactions to improve the selectivity. One such strategy has been to prepare a heterojunction formed between two different single-phase semiconducting ceramic materials, a concept that was first proposed in 1979 for humidity detection.[10] Subsequently the responses of several different heterojunction sensors to a range of target gases including CO, H_2, H_2O, NO_2 and C_2H_5OH have been investigated.[9,11–18]

Geometrically, a heterojunction gas sensor consists of two semiconducting oxides in contact, with the reactions giving rise to the enhanced sensing behaviour occurring at the interface between the two materials. Gases that are adsorbed onto the sensor surface on either side of the heterojunction modify its charge-

* Corresponding author. Tel.: +44-161-200-3561; fax: +44-161-200-3586.
E-mail address: colin.leach@man.ac.uk (C. Leach).

0955-2219/03/$ - see front matter © 2003 Elsevier Science Ltd. All rights reserved.
doi:10.1016/S0955-2219(02)00429-6

transfer characteristics by changing the structure of the interfacial barrier.[12] This process gives rise to a gas detection mechanism distinct from that of single-phase ceramic sensors.

Several systems have been proposed for heterojunction sensors, mostly based on rectifying junctions formed between p-type (p) and n-type (n) semiconducting ceramics, including CuO(p)/ZnO(n),[13,14] La_2CuO_4(p)/ZnO(n)[15] and $SmCoO_3$(p)/MO_x(n), where M = Fe, Zn, In, Sn.[18] In addition, the gas sensing properties of heterojunctions formed between two n-type semiconducting ceramics with slightly different band energies, giving rise to an n–N interface, have also been reported.[16,17] For example, a gas sensor based on a heterojunction formed between the n-type ceramics SiC and ZnO was investigated.[16] The interface was found to be rectifying and the forward bias current (defined by connecting the positive terminal to SiC) decreased on introduction of NO_2. Since the resistance of the SiC component of the heterojunction was unaffected by the introduction of NO_2 and that of the ZnO component was only slightly affected, it was concluded that the increase in electrical resistance associated with the introduction of the NO_2 was due to the behaviour of the n–N heterojunction interface.

In a subsequent study a n–N heterojunction gas sensor was prepared by co-firing n-type ZnO and SnO_2 layers.[17] When exposed to 200 ppm CO, the ZnO/SnO_2 heterojunction sensor showed higher sensitivity than either the ZnO or the SnO_2 components on their own. As the sample thickness was decreased, greater resistivity changes and higher overall sensitivities to CO were observed, leading the workers to conclude that the behaviour of the heterojunction interface was dominant in determining the gas sensitivity of the overall sensor.

Recently the electrical structure of a heterojunction gas sensor interface, formed between CuO and ZnO, was investigated using conductive mode microscopy.[19] At points of contact between the CuO and the ZnO grains, contrast indicative of a locally resistive barrier was observed together with electron beam induced current (EBIC) contrast characteristic of a p–n junction, making it possible to attribute the observed rectifying behaviour to the presence of an interfacial depletion region.

NO_2 is a common air pollutant that is associated, even at the ppb level, with poor air quality and breathing difficulties, particularly in children and the elderly. Both SnO_2[20,21] and WO_3[8,22–26] have been studied as potential single-phase NO_2 sensors and have shown good sensitivity, although in both cases there are still issues of sensitivity, selectivity and long-term stability. Since many workers perceive heterojunction type gas sensors to have inherent advantages that may overcome limitations exhibited by single component gas sensors,[9,13,14,17] a detailed programme of investigations based on the sensing behaviour of heterojunctions is being undertaken. In this context, the SnO_2/WO_3 system has been identified as showing considerable potential. In this contribution, the NO_2 sensitivity and stability of an n–N type heterojunction sensor, formed between WO_3 and 3 wt.% Nd_2O_3 doped SnO_2 is presented, and compared with that of single-phase sensors formed from each of the component materials.

2. Experimental procedure

All of the experiments described in this study were carried out on sensors formed from partially sintered (bulk) pellets. The WO_3 sensor was prepared from GPR grade WO_3 powder, which was compacted and partially sintered at 1000 °C for 5 h to produce a 10 mm diameter pellet. The 3 wt.% Nd_2O_3 doped SnO_2 sensor was prepared by ball milling GPR grade Nd_2O_3 and SnO_2 powders, mixed in the appropriate ratio, in propan-2-ol, followed by drying, compaction and partial sintering at 800 °C for 5 h to produce a 10 mm diameter pellet.

The doped SnO_2 and WO_3 pellets so produced were characterized using a Phillips 525 scanning electron microscope (SEM) and by X-ray diffraction (XRD) using a Phillips X'pert APD diffractometer. The densities of the sintered pellets were determined from measurements of specimen weight and dimensions and their effective surface areas were established using the B.E.T. method.

Prior to the assessment of the electrical and gas-sensing properties, fresh pellet surfaces were exposed by roughening the as-fired faces using 1200-grade silicon carbide paper. For the electrical characterisation of the WO_3 and the doped SnO_2 sensors, silver electrodes were screen-printed onto opposite faces of the pellet and Pt lead-out wires attached (Fig. 1a). The heterojunction sensor was prepared by mechanically clamping together faces of the constituent pellets that had again been roughened to facilitate gas penetration along the interface (Fig. 1b). To assess sensor performance, the specimens were housed in a controlled atmosphere worktube mounted inside a remotely programmable furnace (Fig. 2). For atmosphere control, compressed air was used as a carrier gas to which 0–10 ppm NO_2 was added whilst maintaining a constant overall flow rate of 90 $cm^3\ min^{-1}$.

DC measurements of sensor behaviour were carried out using a Thurlby 6512 voltage source and a Black Star 4503 Intelligent Multimeter, both of which were fitted with an IEEE interface to permit automatic data logging via a computer. AC impedance spectroscopy was performed on the heterojunction sensor in air and in NO_2 using a HP 4192A LF Impedance Analyser operating in the frequency range 5 Hz to 13 MHz and using a forward bias voltage of 0.5 V.

3. Results and discussion

3.1. Microstructure

Fig. 3a is a secondary electron (SE) image of the roughened surface of a 3 wt.% Nd_2O_3 doped SnO_2 sensor, showing a highly porous structure in which particles of around 0.05 μm diameter are loosely bound in agglomerates approximately 5 μm in diameter. The sample density was 2.57 g cm^{-3} or 37% of theoretical and the effective surface area of the sensor, measured using the BET method, was 4.3 m^2 g^{-1}. XRD analysis of the sensor revealed the presence of some residual Nd_2O_3 indicating only partial incorporation into the SnO_2 during the preparation phase.

Fig. 3b shows a SE image of the abraded surface of a sintered WO_3 sensor, which comprises loosely sintered, faceted grains with a mean size of about 1.5 μm. The density of the sample was 4.19 g cm^{-3} or 58% of theoretical, with an effective surface area of 0.7 m^2 g^{-1}.

The heterojunction formed between these n-type materials showed rectifying characteristics, similar to that of a Schottky diode, with a rapid increase in current occurring under forward bias (defined as WO_3 positive), and a small reverse bias leakage current (Fig. 4). Rectifying behaviour has also been reported in a n–N heterojunction sensor based on SnO_2/ZnO.[17] The authors suggested that the rectifying behaviour was brought about by distortions in the band structure due to differences in the electron affinities of the SnO_2 and the ZnO. In the case of the SnO_2/WO_3 heterojunction studied here, it is proposed that the rectifying behaviour is caused by a similar mechanism.

3.2. DC response of the sensors

3.2.1. Single component sensors

Fig. 5 shows the response of a Nd_2O_3 doped SnO_2 sensor operating at 300 °C to 3 ppm NO_2. Under a carrier gas of dry compressed air the sensor maintains a stable, baseline resistivity of 501 MΩ cm. After introducing 3 ppm NO_2 to the carrier gas, the sensor resistivity increases to around 1730 MΩ cm, fully stabilising in about 15 h. On reverting to dry air the resistivity returned to 501 MΩ cm in about 5 h.

Fig. 6 shows the response of a WO_3 sensor to two cycles of 1.5 ppm NO_2 at 300 °C. During each cycle the sensor resistivity increases from 1.15 MΩ cm in air to 2.60 MΩ cm in NO_2, fully stabilising in about 5 h. When the NO_2 is turned off, the resistivity of the WO_3 sensor reverts to the 'air' value in about 2 h.

Since both SnO_2 and WO_3 show n-type behaviour, the resistivity increase associated with the introduction of the NO_2 may simply be explained in terms of an increase in the height of electrostatic grain boundary barriers, which form initially due to the surface adsorption and ionisation of oxygen molecules. When NO_2 is introduced into the surrounding atmosphere, it too is adsorbed on the surface of the sensor and adopts a stable anionic form[26,27] by capturing electrons from the bulk, leading to a further increase in the grain boundary barrier height, which results in the observed increase in grain boundary resistance. A recent AC impedance

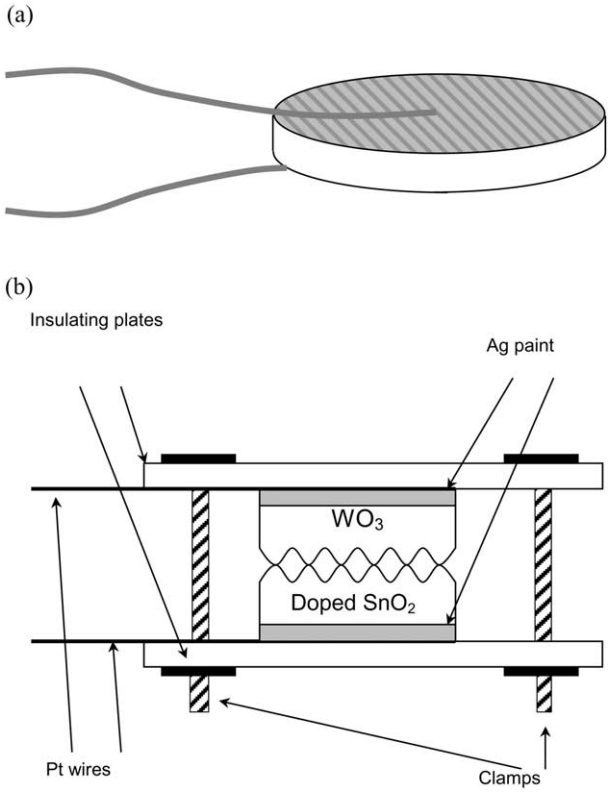

Fig. 1. The sample configurations used to test (a) the single pellet sensors, and (b) the heterojunction sensor.

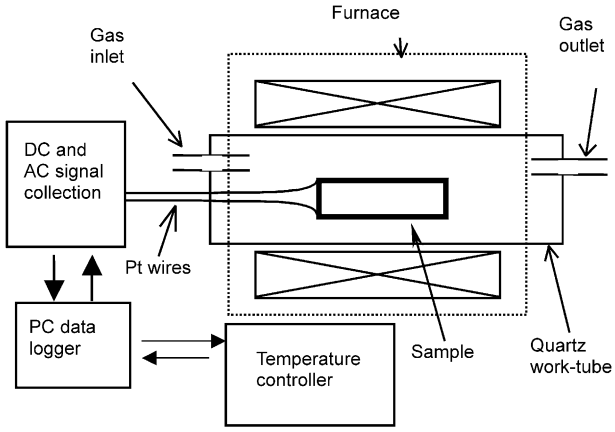

Fig. 2. Schematic diagram showing the controlled atmosphere furnace and data collection system.

study of the transient response of a WO_3 based sensor to 1.5 ppm NO_2[28] established that the change in sensor resistivity due to the introduction of NO_2 was the result of an increase in grain boundary barrier height from 212 m eV in air to 291 me V in NO_2.

3.2.2. Heterojunction sensor

The single component sensors, whose performances were described in the previous section, were reassembled to form a heterojunction sensor for testing. Fig. 7 shows the response of this heterojunction sensor when exposed

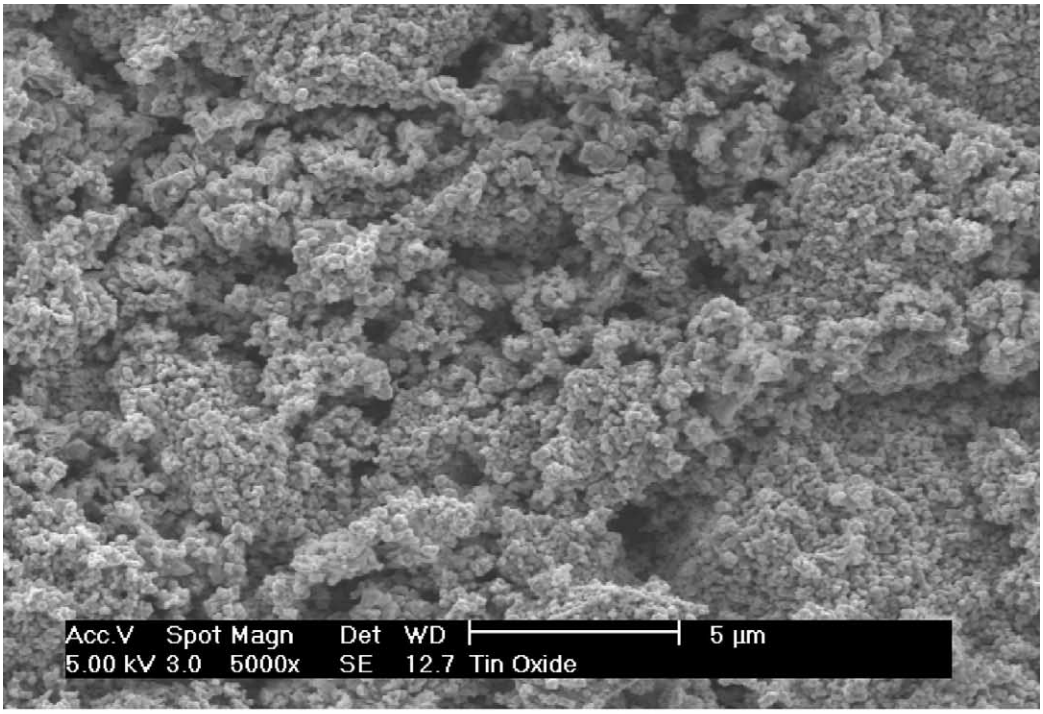

(a)

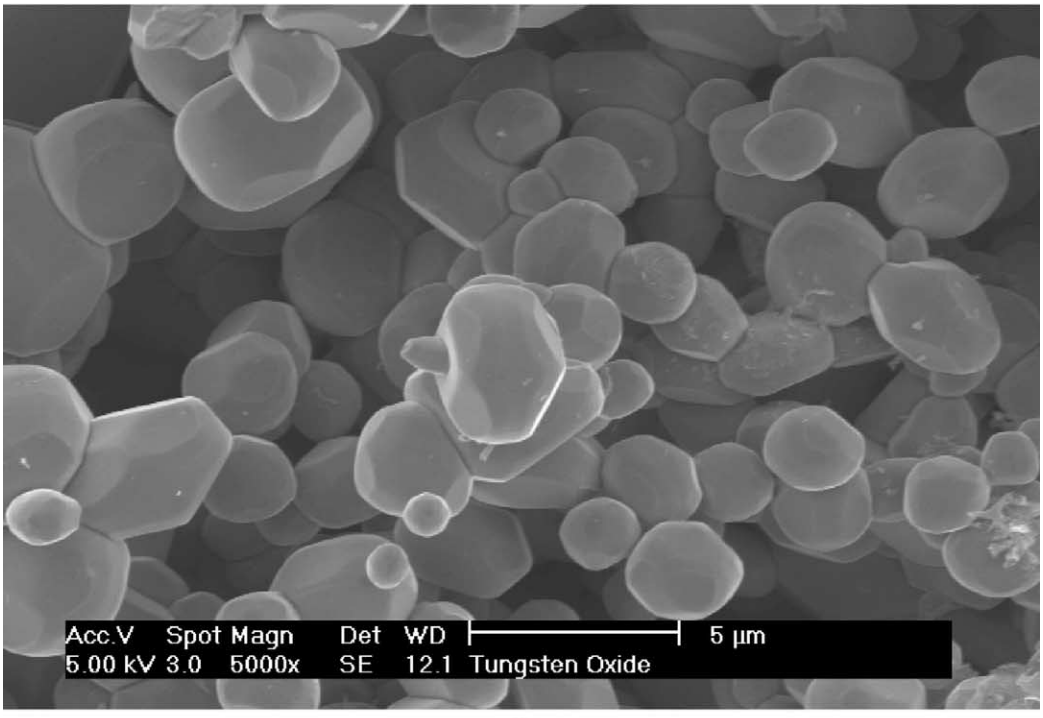

(b)

Fig. 3. (a) SEM image of the ground surface of a 3 wt.% Nd_2O_3 doped SnO_2 sensor sintered at 800 °C for 5 h; (b) SEM image of the ground surface of the WO_3 sensor sintered at 1000 °C for 5 h. Scale bars = 5 µm.

to different levels of NO_2 in the range 0–10 ppm at 300 °C. The equilibrium resistivity increases from 3.4 MΩ cm in air to 10 MΩ cm, 17.4 MΩ cm and 209 MΩ cm in atmospheres containing 1, 1.5 and 10 ppm NO_2 respectively. The sensor response was fully reversible in this concentration range, re-equilibration to increased NO_2 levels typically took 15 h whereas re-equilibration to lower NO_2 levels took 5 h.

The response time of the heterojunction sensor to NO_2 is similar to that of the component SnO_2 sensor and both are longer than that of the WO_3 sensor. This indicates that the rate of sensor response is determined by reactions occurring at the heterojunction interface, since the rate-determining step in controlling the response time of the heterojunction sensor is determined by the slower response of the SnO_2 based element.

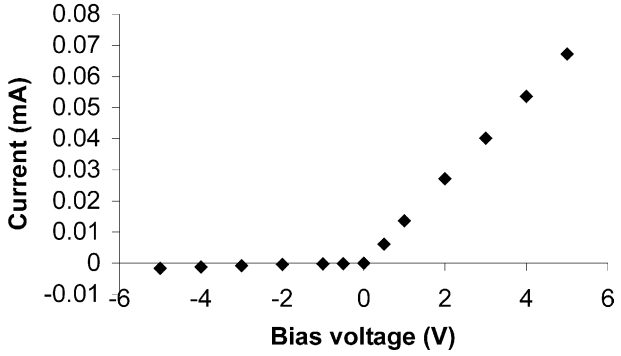

Fig. 4. Current–voltage (I–V) characteristics of a 3 wt.% Nd_2O_3 doped SnO_2/WO_3 heterojunction sensor at 300 °C in dry air, showing rectifying behaviour.

A quantitative comparison of the sensitivities of the heterojunction sensor and its component elements was carried out by measuring the responses of the doped SnO_2 and WO_3 sensors to NO_2 in the range 0–5 ppm at 300 °C and then comparing these with the response of the heterojunction formed by bringing the two constituent elements together. In this way any difference between the overall resistance of the heterojunction in different atmospheres and the sum of the individual sensors' resistances could be observed and characterised.

Prior to testing, each sensor was conditioned at 300 °C under a carrier gas of dry air flowing at 90 cm^3 min^{-1}, until a stable baseline resistance value in air, R_{air}, was established. NO_2 was then introduced at specific concentrations in the range 0–5 ppm and the resistance monitored, again until a stable value was obtained. The results so obtained are presented in Table 1. It can be seen that, with increasing NO_2 concentration, an increasing discrepancy exists between the resistance of the heterojunction (R_{HJ}) and the sum of the resistances of the doped SnO_2 (R_{SnO_2}) and the WO_3 (R_{WO_3}) sensors, suggesting that another resistive element, presumably arising from the behaviour of the doped SnO_2–WO_3 interface, contributes to the overall resistance of the heterojunction sensor. Although the resistances of the bulk SnO_2 and WO_3 both increase when NO_2 is introduced and contribute to the total resistance increase of the sensor, the extra resistance, given by the difference between R_{HJ} and ($R_{SnO_2} + R_{WO_3}$), is the major contribution to the overall resistance of the heterojunction sensor when exposed to NO_2. Since this additional

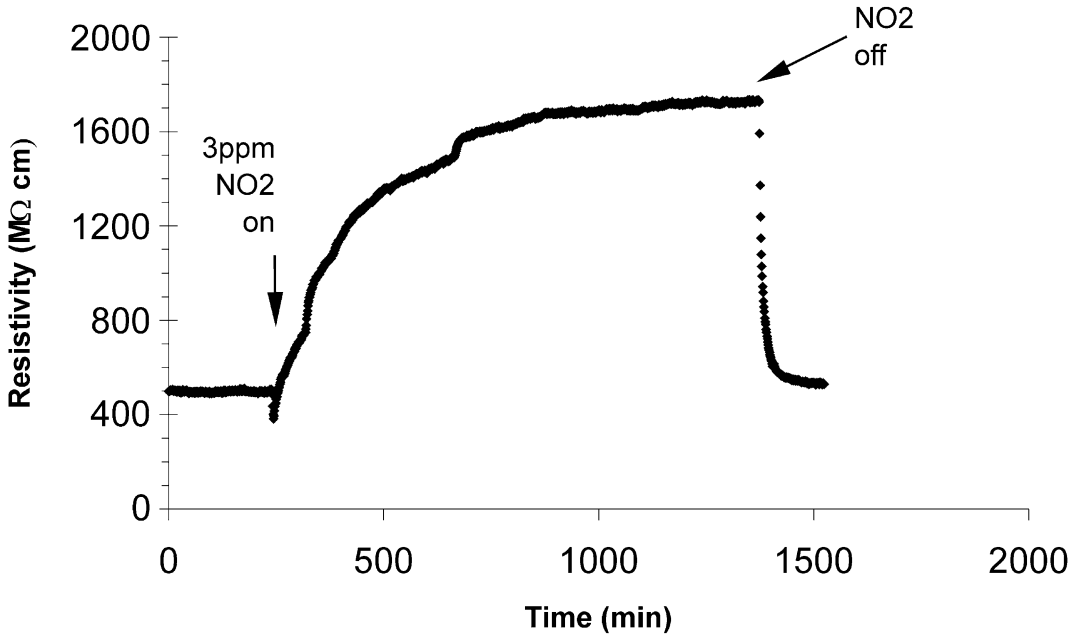

Fig. 5. Response of the 3 wt.% Nd_2O_3 doped SnO_2 sensor to 3 ppm NO_2 at 300 °C.

contribution is attributed to the interfacial resistance of the heterojunction, it has been termed R_{int} (Table 1).

In order to quantify the relative responses of the heterojunction and its component sensors, a sensitivity coefficient, M, was calculated for each sensor at each NO_2 concentration using the relationship:

$$M = R_{NO_2}/R_{air} \quad (2)$$

where R_{NO_2} is the resistance of a given sensor at a given NO_2 concentration and R_{air} the sensor resistance in air. The data so obtained are shown in Fig. 8. It is noted that the value of M, calculated for each of the sensors, increases linearly with increasing NO_2 concentration, with correlation coefficient (R^2) values as shown in Table 2. Further, for all NO_2 concentrations, the value of M calculated for the heterojunction sensor is greater than the M values of the individual single component sensors. The sensitivities of each of the sensors, defined as change in M per ppm change in NO_2 concentration were determined from the gradients of the graphs in Fig. 8 and are also listed in Table 2. The NO_2 sensitivity of the heterojunction sensor is almost an order of magnitude greater than those of the component sensors. Since this high NO_2 sensitivity cannot be explained in terms of an accumulation of the responses of the component sensors, it is proposed that the improved sensitivity be attributed to the performance of the heterojunction interface.

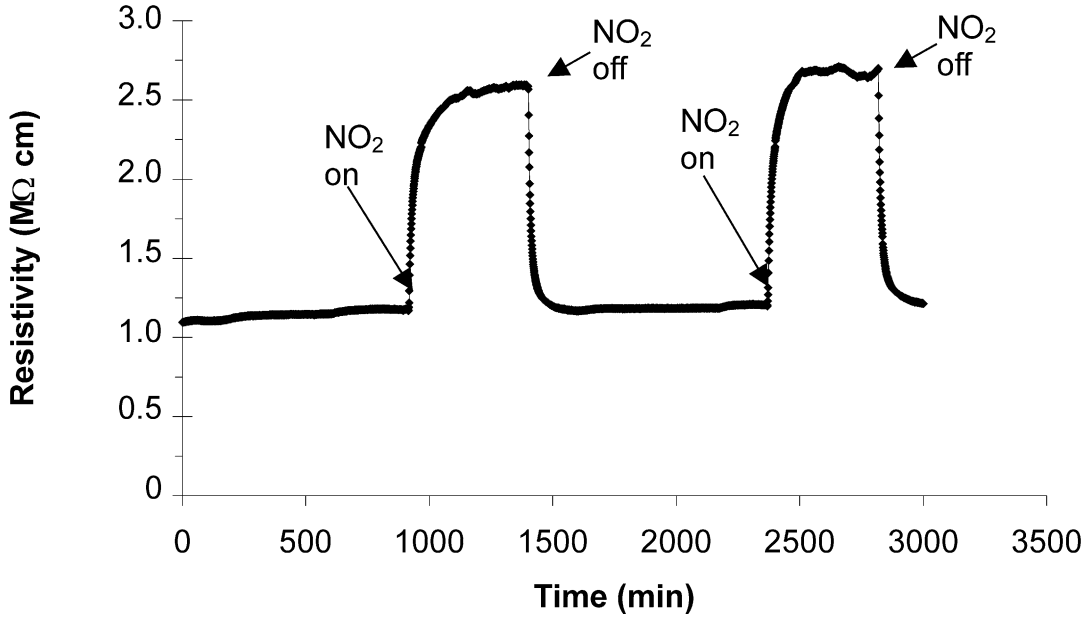

Fig. 6. Time resolved response of the WO_3 sensor to 1.2 ppm NO_2 at 300 °C.

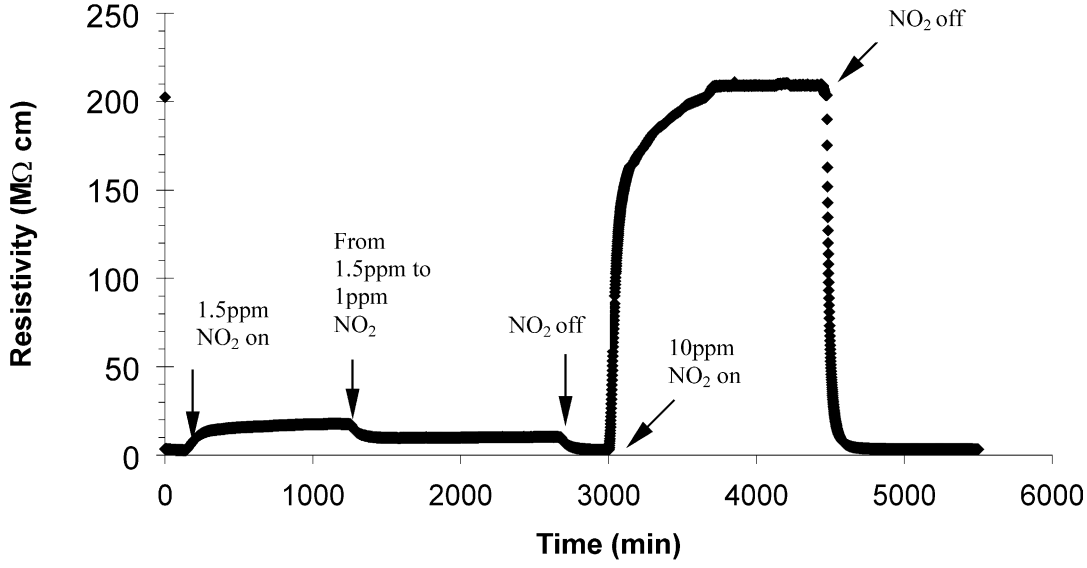

Fig. 7. Response of a 3 wt.% Nd_2O_3 doped SnO_2/WO_3 heterojunction sensor to 1.5, 1 and 10 ppm NO_2 at 300 °C.

A series of I–V measurements was performed on the heterojunction sensor at 300 °C using applied voltages in the range −5V to +5V, and NO_2 concentrations in the range 0–5 ppm (Fig. 9). In all of the tests, the sensor showed rectifying behaviour with the forward bias current (defined as WO_3 positive) decreasing as the NO_2 concentration was increased. The reverse bias current remained negligible and almost unchanged under all gas conditions.

Table 1
DC resistances of the component (R_{SnO_2}, R_{WO_3}) and heterojunction (R_{HJ}) sensors to NO_2 at 300 °C, and the corresponding resistances (R_{int}) attributed to the heterojunction interface

NO_2 concentration (ppm)	R_{SnO_2} (kΩ)	R_{WO_3} (kΩ)	R_{HJ} (kΩ)	R_{int} (kΩ)
0 (air)	779	70	913	64
1	1490	139	8330	6701
1.5	1750	181	12 900	10 969
2	2100	208	16 700	14 392
3	2720	296	23 300	20 284
3.5	2930	315	27 800	24 555
5	3860	412	39 400	35 128

The bias dependence of sensitivity of the sensor is shown in Fig. 10, in terms of the percentage change in forward bias current (ΔI) as a function of forward bias voltage (0.5 V, 3 V and 5 V), and was calculated according to:

$$\Delta I = 100 \times \left(I_{air} - I_{NO_2}\right)/I_{air} \quad (1)$$

where I_{air} is the current at a given bias in air, and I_{NO_2} the corresponding current in NO_2. For each level of bias the current increased linearly with increasing NO_2 concentration. The sensitivity, defined as the change in current per ppm increase in NO_2 concentration and given by the gradients of these curves, decreased only slightly with increasing bias voltage and so it is con-

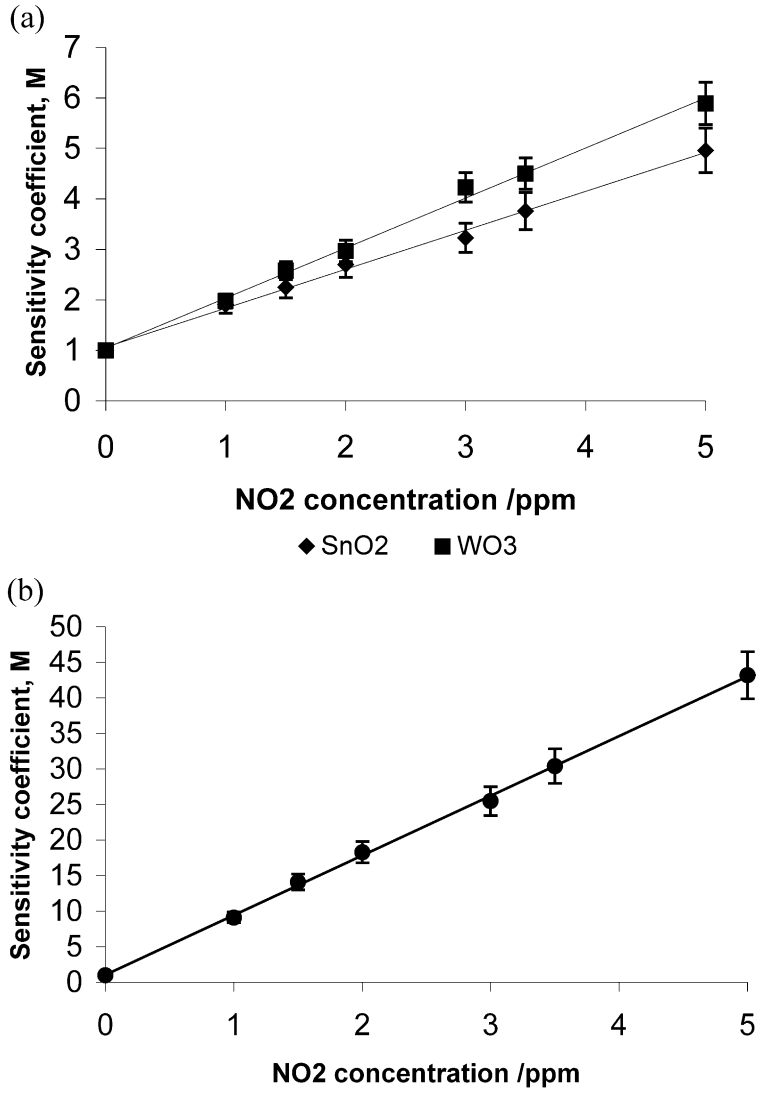

Fig. 8. Response size and sensitivity of the sensors in the range 0–5 ppm NO_2 at 300 °C. (a) the 3 wt.% Nd_2O_3 doped SnO_2 and WO_3 sensors, (b) the heterojunction sensor.

cluded that the sensitivity of the sensor studied here did not show a significant bias dependence. This behaviour contrasts with observations made in other systems. For example a study of a sensor based on a La_2CuO_4/ZnO heterojunction revealed a strong bias dependence of sensitivity to humidity with a peak sensitivity occurring when 2.5 V forward bias was applied.[29,30] In this case, increasing the target gas concentration resulted in a decrease in the interfacial resistance; behaviour that was attributed to an electrolytic breakdown mechanism.

The weak bias dependence of the NO_2 response in the system reported here, coupled with an increase in the overall sensor resistance on exposure to NO_2, suggests that sensing via an electrolytic breakdown mechanism is not appropriate in this case. It is proposed instead that the response to NO_2 reported here is principally due to changes in the electrostatic barrier height at the heterojunction interface brought about by a surface build-up of charge arising from the ionisation of adsorbed NO_2. The effect on the sensor resistance of this barrier height increase is greater than that of the WO_3 or the doped-SnO_2 component elements individually, and may be due to the presence of more effective NO_2 bonding sites at the interface permitting a greater surface concentration of NO_2 or a locally increased density of trap states permitting a higher electrostatic barrier to form. In these circumstances the time taken for the barrier to stabilise, and hence the response time of the heterojunction interface, would be governed by the performance of the slower element, namely the doped-SnO_2.

Finally it is noted that the sensor geometry used here requires that all current must pass through the heterointerface, and so it is likely that a sensor in this form would display a stronger interface effect than sensors prepared in other ways such as a duplex mix of the same component phases, where percolating networks of the two components would exist in parallel and dilute the influence of the interface.

Table 2
Sensitivity values and linearity coefficients (R^2) for the single phase and heterojunction sensors to NO_2 at 300 °C

Sensor	NO_2 sensitivity	R^2
Doped SnO_2	0.77 (ppm NO_2) + 1	0.9958
WO_3	0.99 (ppm NO_2) + 1	0.9959
Heterojunction	8.4 (ppm NO_2) + 1	0.9991

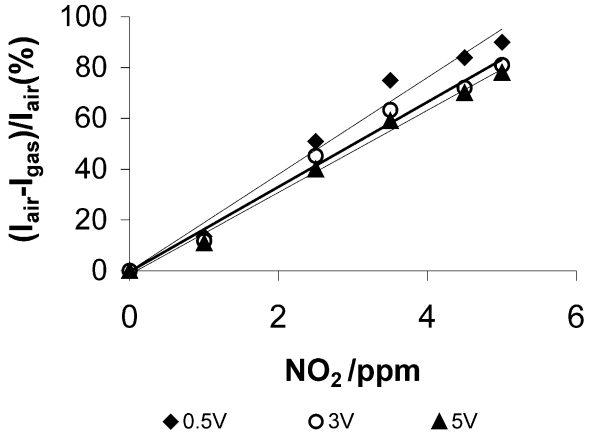

Fig. 10. Sensitivity of the heterojunction sensor in the range 0–5 ppm NO_2 at 300 °C and 0.5, 3 and 5 V forward bias.

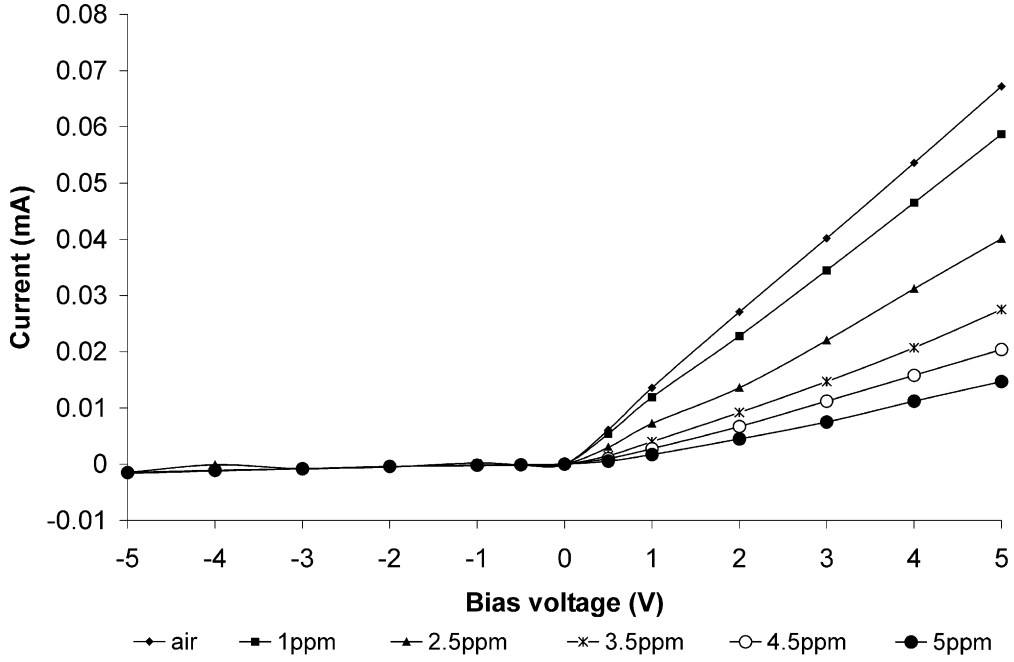

Fig. 9. I–V characteristics of a heterojunction sensor at 300 °C under NO_2 concentrations in the range 0–5 ppm.

3.3. AC impedance analysis of the SnO_2/WO_3 heterojunction sensor

AC impedance spectroscopy provides frequency resolved information that is able to resolve the contributions of different component regions (e.g. bulk, grain boundary, electrode) to the total electrical properties of electroceramics through differences in the time constants of each element.[31] In this work a preliminary AC impedance spectroscopy study was performed on the heterojunction sensor in an attempt to gain more information about changes occurring at the heterojunction interface on introduction of NO_2, by comparing the responses in air and after stabilisation in 2.5 ppm NO_2 at 300 °C. Nyquist plots revealed two semicircles corresponding to separate relaxations in both the air equilibrated (Fig. 11a) and the 2.5 ppm NO_2 equilibrated (Fig. 11b) spectra. The inset in Fig. 11b shows in detail the overlapping high frequency relaxation.

From the DC measurements in air (Table 1) it can be seen that R_{int} is smaller than R_{SnO_2} and R_{WO_3} and so the relaxations visible in Fig. 11a are attributed to overlapping responses form the individual WO_3 and SnO_2 elements. After equilibration in NO_2, R_{int} increases dramatically, resulting in the large relaxation in Fig. 11b, from which the interfacial capacitance is estimated to be 180 pF. A detailed study of the transient response of the heterojunction sensor is currently underway.

3.4. Stability of the heterojunction sensor

The long-term stability of the heterojunction sensor was evaluated over a period of 56 days continuous running at 300 °C in an atmosphere whose NO_2 concentration varied

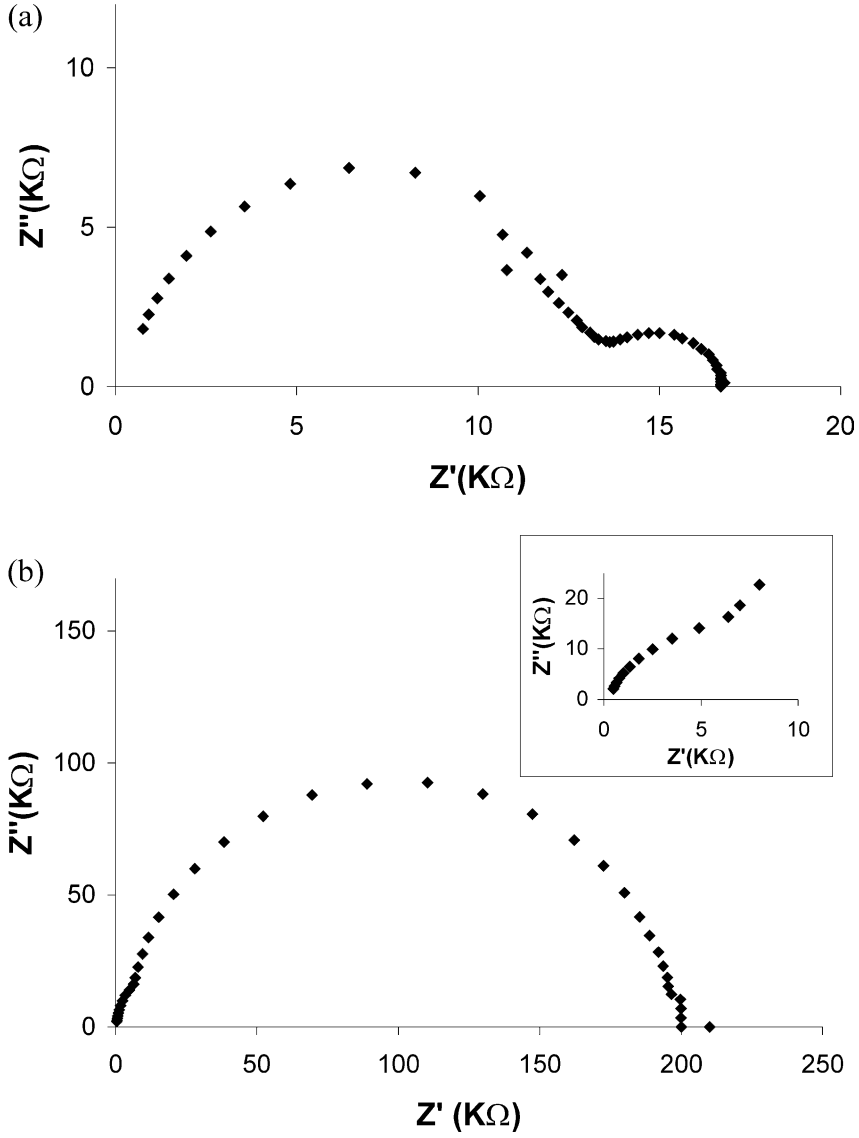

Fig. 11. Nyquist plots of the heterojunction sensor at 300 °C (a) in air, and (b) 2.5 ppm NO_2.

periodically in the range 0–10 ppm. Table 3 lists values of sensor resistance measured after equilibration at various NO_2 concentrations during the test. The 'air' resistance of the sensor remained consistent throughout the test period, lying in the range 13–14 kΩ. On introducing NO_2 over a range of concentrations the sensor resistance increased over the air value, reproducibly reaching new equilibrium values for each level of NO_2. The measured values were consistent with the responses recorded in Fig. 9 in the range 0–5 ppm. However the resistance measured after introducing 10 ppm NO_2 was lower than a linear extrapolation of the Fig. 9 data would suggest, indicating that the response of the sensor may be beginning to saturate at this concentration level. On removing the NO_2 from the gas flow the resistance value of the sensor always returned to its initial base-line value of 13–14 kΩ in air.

This consistency of performance over an extended period indicates that the gas sensing reaction is fully reversible at 300 °C, and that the sensor is a strong candidate for long term sensing applications. Although the sluggishness of response precludes its use in alarm applications, it shows considerable potential for integrated long term monitoring of background NO_2 levels in environmental or industrial situations.

Table 3
Resistance change of a SnO_2/WO_3 sensor at 300 °C and the calculated response size to variation of NO_2 concentration

Day	Gas condition	Resistance (kΩ)	R_{gas}/R_{air}
1	Air	13.3	
3	Air + 2 ppm NO_2	121.4	9.05
6	Air	13.1	
10	Air + 2 ppm NO_2	123.2	9.19
13	Air	12.9	
15	Air + 5 ppm NO_2	570.3	42.5
16	Air	13.4	
18	Air + 5 ppm NO_2	575.2	42.9
20	Air	13.6	
22	Air + 3.3 ppm NO_2	209	15.6
23	Air	13.8	
24	Air + 2 ppm NO_2	125.3	9.34
26	Air + 1.7 ppm NO_2	70.8	5.4
27	Air + 1.7 ppm NO_2	69.3	5.17
28	Air + 0.9 ppm NO_2	41.2	3.07
29	Air	13.9	
30	Air + 10 ppm NO_2	814	60.7
32	Air	13.9	
33	Air + 5 ppm NO_2	572	42.7
35	Air + 3.3 ppm NO_2	212	15.8
37	Air + 1.7 ppm NO_2	71.2	5.31
39	Air	13.8	
45	Air + 2 ppm NO_2	122.6	9.36
50	Air	13.6	
53	Air + 5 ppm NO_2	574.8	42.83

4. Conclusions

The response of a novel heterojunction gas sensor, formed from low-cost starting materials, between WO_3 and a 3 wt.% Nd_2O_3 doped SnO_2 pellets, was evaluated by characterising the DC and AC responses to NO_2 in dry air. This new n–N type heterojunction sensor was found to show improved NO_2 sensitivity compared with the responses of the component WO_3 and 3 wt.% Nd_2O_3 doped SnO_2 sensors. This improved response is believed to be due to the formation of an enhanced electrostatic barrier at the heterojunction interface, associated with the adsorption of NO_2.

The heterojunction sensor was found to show a linear, stable and reproducible response to NO_2 in the range 0–5 ppm, with little or no drift observable after 56 days continuous operation.

Acknowledgements

Support from EPSRC Grant GR/M33525 is acknowledged.

References

1. Brattain, W. H. and Bardeen, J., Surface properties of germanium. *Bell. Syst. Tech. J.*, 1953, **32**, 1.
2. Sanjines, R., Levy, F., Demarneand, V. and Grisel, A., Some aspects of the interaction of oxygen with polycrystalline SnO_x thin-film. *Sens. Actuators B*, 1990, **1**, 176–182.
3. Demarne, V., Grisel, A., Sanjines, R., Rosenfeld, D. and Levy, F., Electrical transport-properties of thin polycrystalline SnO_2 film sensors. *Sens. Actuators B*, 1992, **6-7**, 704–708.
4. Moseley, P. T. and Williams, D. E., A selective ammonia sensor. *Sens. Actuators B*, 1990, **1**, 113–115.
5. Seiyama, T., *Chemical Sensor Technology*, Vol. 1, ed. T. Seiyama. Elsevier, 1988, p. 1.
6. Heiland, G. and Kohl, D. *Chemical Sensor Technology*, Vol. 1, ed. T. Seiyama. Elsevier, 1988, p. 15.
7. Moseley, P.T. and Tofield, B.C. (eds), *Solid State Gas Sensors*. IOP Publishing Ltd., 1987.
8. Akiyama, M., Tamaki, J., Miura, N. and Yamazou, N., Tungsten oxide-based semiconductor sensor highly sensitive to NO and NO_2. *Chemistry Letters*, 1991, **9**, 1611–1614.
9. Traversa, E., Design of ceramic materials for chemical sensors with novel properties. *J. Am. Ceram. Soc.*, 1995, **78**, 2625–2632.
10. Kawakami, K. and Yanagida, H., *J. Ceram. Soc. Jpn*, 1979, **87**, 112–115.
11. Yanagida, H., Intelligent ceramics. *Ferroelectrics*, 1990, **102**, 251–257.
12. Hikita, K., Miyayama, M. and Yanagida, H., New approach to selective semiconductor gas sensors using a DC-biased *p-n* heterocontact. *J. Am. Ceram. Soc.*, 1995, **78**, 865–873.
13. Jung, S. J., Ohsawa, H., Nakamura, Y., Yanagida, H., Hasumik, K. and Okada, O., Effects of Na_2O_3 addition on the gas sensing characteristic of CuO/ZnO heterocontact. *J. Electrochem. Soc.*, 1994, **141**, 53–55.
14. Jung, S. J. and Yanagida, H., The characterisation of CuO/ZnO heterocontact type gas sensor having selectivity for CO gas. *Sens. Actuators B*, 1996, **37**, 55–60.

15. Traversa, E., Miyayama, M. and Yanagida, H., Gas sensitivity of ZnO/La_2CuO_4 heterocontacts. *Sens. Actuators B*, 1994, **17**, 257–261.
16. Nakamura, Y., Koyama, R., Koumoto, K. and Yanagida, H., Oxidizing gas sensing by SiC/ZnO heterocontact-NOx sensing. *J. Ceram. Soc. Jpn*., 1991, **99**, 823–825.
17. Yu, J. H. and Choi, G. M., Electrical and CO gas-sensing properties of ZnO/SnO_2 hetero-contact. *Sens. Actuators B*, 1999, **61**, 59–67.
18. Mochinaga, R., Yamasaki, T. and Arakawa, T., The gas-sensing of SmCoOx/MOx (M = Fe,Zn,In,Sn) having a heterojunction. *Sens. Actuators B*, 1998, **52**, 96–99.
19. Leach, C., Ling, Z. and Freer, R., Direct observation of the barrier structure in a heterojunction gas sensor using conductive mode microscopy. *Scripta Mater*., 2000, **42**, 1083–1088.
20. Chiorino, A., Ghiotti, G., Prinetto, F., Carotta, M. C., Malagu, C. and Martinelli, G., Preparation and characterization of SnO2 and WOx-SnO2 nanosized powders and thick films for gas sensing. *Sens. Actuators B*, 2001, **78**, 89–97.
21. Karthigeyan, A., Gupta, R. P., Scharnagl, K., Burgmair, M., Zimmer, M., Sharma, S. K. and Eisele, I., Low temperature NO_2 sensitivity of nano-particulate SnO_2 film for work function sensors. *Sens. Actuators B*, 2001, **78**, 69–72.
22. Cantalini, C., Sun, H. T., Faccio, M., Pelino, M., Santucci, S., Lozzi, L. and Passacantando, M., NO_2 sensitivity of WO_3 thin film obtained by high vacuum thermal evaporation. *Sens. Actuators B*, 1996, **31**, 81–87.
23. Sberveglieri, G., Depero, L. and Groppelli, S., WO_3 sputtered thin films for NO_x monitoring. *Sens. Actuators, B*, 1995, **26**, 89–92.
24. Cantalini, C., Pelino, M., Sun, H. T., Faccio, M., Santucci, S., Lozzi, L. and Passacantando, M., Cross sensitivity and stability of NO_2 sensors from WO_3 thin film. *Sens. Actuators B*, 1996, **35**, 112–118.
25. Lee, D. S., Lim, J. W., Lee, S. M., Huh, J. S. and Lee, D. D., Fabrication and characterization of micro-gas sensor for nitrogen oxides gas detection. *Sens. Actuators B*, 2000, **64**, 31–36.
26. Chung, Y. K., Kim, M. H., Um, W. S., Lee, H. S., Song, J. K., Choi, S. C., Yi, K. M., Lee, M. J. and Chung, K. W., Gas sensing properties of WO_3 thick film for NO_2 gas dependent on process condition. *Sens. Actuators B*, 1999, **60**, 49–56.
27. Walter, C. W., Hertzler, C. F., Devynck, P., Smith, G. P. and Peterson, J. R., Photodetachment of WO_3- the electron-affinity of WO_3. *J. Chem. Phys*., 1991, **95**, 824–827.
28. Ling, Z., Leach, C. and Freer, R. A time resolved study of the response of a WO_3 gas sensor to NO_2 using AC impedance spectroscopy. *Sens. Actuators B* (in press).
29. Traversa, E., Bearzotti, A., Miyayama, M. and Yanagida, H., The electrical properties of La_2CuO_4/ZnO heterocontacts at different relative humidities. *J. Mater. Res*., 1995, **10**, 2286–2294.
30. Hikita, K., Miyayama, M. and Yanagida, H., CO gas identification by use of complex impedance of p-n heterocontact comprising of Na-added CuO and ZnO. *J. Ceram. Soc. Jpn*., 1994, **102**, 810–817.
31. Bauerle, J. E., Study of a solid electrolyte polarisation by a complex admittance method. *J. Phys. Chem. Solids*, 1969, **30**, 2657–2670.